Frontiers in Bioscience Scholar

*Front. Biosci. (Schol Ed)* **2026**; 18(3): 48977
https://doi.org/10.31083/FBS48977

*Original Research*

# Biochemical Characterization of Ribonuclease Activities From the Sea Cucumber *Eupentacta fraudatrix*

Svetlana E. Soboleva[1,*,†], Valeria A. Ivaschenko[1,†], Irina A. Kostrikina[1], Georgy A. Nevinsky[1]

[1]Institute of Chemical Biology and Fundamental Medicine, Siberian Division of Russian Academy of Sciences, 630090 Novosibirsk, Russia
*Correspondence: lactofer@mail.ru (Svetlana E. Soboleva)
[†]These authors contributed equally.

Academic Editor: Gustavo Caetano-Anollés
Submitted: 10 December 2025 Revised: 4 February 2026 Accepted: 13 February 2026 Published: 15 July 2026

**Abstract**

**Background**: The sea cucumber *Eupentacta fraudatrix* is a highly interesting model organism for research due to the remarkable ability of the organism to regenerate lost organs following evisceration. In animals after evisceration, increased expression levels of genes such as *Sox* (SRY-related HMG-box, transcription factors), *MMP* (matrix metalloproteinases), *TIMP* (tissue inhibitors of metalloproteinases), and *PIWI* (ribonuclease-active proteins) have been observed. Since ribonucleases release nucleotides for the synthesis of new molecules and regulate cellular processes by acting on various RNA species, these enzymes are hypothesized to play a significant role in regeneration. **Methods**: Holothurian homogenate was fractionated chromatographically into several protein fractions. Ribonuclease activity was analyzed using a specific microRNA (miRNA) as a substrate, as well as by an in-gel activity assay. **Results**: This study examined the ribonuclease activity of *E. fraudatrix* proteins precipitated with ammonium sulfate from whole-organism homogenates, focusing on pH dependence and substrate specificity. The optimal pH for hydrolyzing a specific miRNA related to the sea cucumber *Apostichopus japonicus* and a non-specific homo-oligonucleotide, $(pA)_{23}$, was 5.0 and 6.0, respectively. Inhibition of ribonuclease activity in the presence of EDTA (ethylenediaminetetraacetic acid), $Mg^{2+}$, and $Ca^{2+}$ indicates dependence on metal ions. Hydrolysis of the specific substrate was about 25% higher than that of the non-specific substrate and produced five cleavage sites. Using in-gel activity analysis, five protein bands with ribonuclease activity were detected in *E. fraudatrix* homogenate, with apparent molecular masses ranging from 15 to 77 kDa. **Conclusions**: This work represents the first report describing the biochemical properties of a ribonuclease from this holothurian species. Five protein forms with ribonuclease activity, differing in electrophoretic mobility, were identified. The biochemical characteristics of these enzymes resemble those of ribonucleases from other echinoderms. Ribonucleases from echinoderms are promising tools for molecular biology applications, including DNA purification, RNA analysis and mapping, as well as for biomedicine, particularly in the development of antiviral agents.

**Keywords:** sea cucumber; *Eupentacta fraudatrix*; RNase; metal-dependent ribonucleases; miRNA

## 1. Introduction

*Eupentacta fraudatrix* is one of the most extensively studied holothurian species in terms of its developmental and regenerative biology [1]. The study also revealed an upregulated expression of specific gene families in the cells of the regenerating digestive system. These include the *Sox* family (SRY-related HMG-box, encoding transcription factors), *PIWI* (multifunctional proteins with RNA-cleaving activity, among other functions), as well as Wnt and Frizzled (key components of multiple signaling pathways) [2,3]. Furthermore, it has been demonstrated that, alongside mRNA, various non-coding RNAs play a critical role during holothurian regeneration. Circular RNAs (circRNAs), long non-coding RNAs (lncRNAs), and miRNAs have been shown to participate in signaling, cell proliferation, migration, and other cellular events during intestinal regeneration [4,5]. Consequently, it may be hypothesized that ribonucleases, by degrading different types of RNA, not only release nucleotides for the synthesis of new molecules required for rapid cell division and differentiation in the regeneration zone but also ensure precise spatiotemporal control over the restoration processes.

RNases, representing a broad class of nucleases, prevent synthesis of mutant proteins by eliminating defective transcripts [6]. Beyond transcript degradation, RNases participate in RNA maturation and translational control [7,8]. Enzymes involved in replication and repair processes also frequently exhibit RNase activity. Among echinoderms, only ribonucleases of the T2-type, isolated from the gonads of sea stars and sea urchins, have been described. These are acidic enzymes (optimal pH 5.0–5.5) with a relatively low molecular mass, ranging from 30 to 40 kDa [9,10]. Despite this broader context, holothurian RNases remain largely uncharacterized. However, transcriptomic analyses of *E. fraudatrix* have revealed dynamic changes during evisceration [11]. Specifically, PIWI protein expression increases in coelomocytes and digestive system cells following evisceration compared to intact animals [2,12]. This protein, like

other members of the evolutionarily conserved Argonaute family, is expressed in pluripotent and multipotent somatic stem cells across invertebrate and vertebrate species, typically in regenerative contexts. PIWI proteins form structural complexes with piRNAs (small non-coding RNAs essential for maintaining pluripotency, transposon silencing, and epigenetic regulation) and exhibit preferential RNA hydrolysis activity [2,12].

MiRNAs represent another class of short non-coding RNAs (18–28 nucleotides) that suppress target gene expression through mRNA binding and degradation or translational inhibition [13,14]. Consequently, miRNAs regulate cellular differentiation, proliferation, migration, apoptosis, homeostasis, and organ regeneration [15,16,17]. While numerous miRNAs have been identified and characterized in various organisms (primarily human), *Apostichopus japonicus* remains the only holothurian species with documented miRNA studies, owing to its commercial importance. miRNA expression patterns in *A. japonicus* alter during skin ulceration [18,19], intestinal regeneration [20,21,22], aestivation [23], and in response to temperature, salinity, and hypoxic stress [24,25,26]. Specific miRNAs (miR-252 family, Aja-miR-2001, Aja-miR-3615, Aja-miR-64d-3p, Aja-miR-3963, Aja-miR-7278-5p, and Aja-miR-1715-5p) have been implicated in intestinal regeneration processes [20]. Notably, Aja-miR-1715-5p (putatively regulating acetylcholinesterase and sushi-domain containing genes) shows >1380-fold upregulation in regenerating intestinal tissue.

Therefore, proteins exhibiting RNase activity likely can play crucial roles in regeneration. Characterization of their properties, including miRNA hydrolysis, could elucidate fundamental mechanisms underlying structural restoration. Ribonucleases derived from echinoderms can be utilized in research for removing RNA from DNA preparations, analyzing RNA structure, performing RNA mapping experiments, and in medicine as antiviral agents to treat diseases caused by RNA-containing viruses. Therefore, this study presents the first investigation and characterization of ribonuclease-active proteins from the sea cucumber *E. fraudatrix*. We determined the pH optimum, metal dependence, and apparent molecular masses of these RNases.

## 2. Materials and Methods

### *2.1 Reagents*

Most chemicals used in this study were provided by Sigma (St. Louis, MO, USA), Superdex 75 HR 10/30 column and Q Sepharose (GE Healthcare Life Sciences, Chicago, IL, USA). *E. fraudatrix* adult sea cucumbers were collected from Peter the Great Bay, Sea of Japan. All holothuria samples were frozen at –42 °C and then stored until the experiment. Fluorescently labeled (fluorescein isothiocyanate; Flu) homo-oligonucleotides 5′-Flu-$(pA)_{23}$ and hetero-oligonucleotide 5′-Flu-miR-aja-1715-5p (5′-Flu-CAGUGCAGGGUCCGAGGUAU) and complementary to them unlabeled ONs were used in the study.

### *2.2 Preparation of E. fraudatrix Sea Cucumber Homogenate*

Given the small size of this species (approximately 3–5 cm in length and 1 cm in diameter), isolating sufficient quantities of individual organs for analysis proved to be a labor-intensive challenge. Therefore, at this stage of the study, whole-organism homogenates of the sea cucumber *E. fraudatrix* were prepared for investigation. Frozen *Eupentacta fraudatrix* specimens (total mass 262 g) were thawed and washed with a three-fold volume of Amphotericin B antibiotic solution. The tissue was then homogenized with lysis buffer (10 mM Tris-HCl, pH 8.0; 1 M NaCl; 1 mM DTT; 1 mM EDTA, pH 8.0; Amphotericin B) in a 1:1.5 (w/v) ratio using a commercial blender. All subsequent procedures were performed on ice. The homogenate was incubated for 1 hour followed by centrifugation at 16,500 ×g for 40 minutes at 4 °C. The supernatant was subjected to ultrasonic treatment (15 cycles of 15 seconds each). The pellet was resuspended in the remaining lysis buffer and extracted for 1 hour, then centrifuged again under the same conditions (16,500 ×g, 40 minutes, 4 °C). The resulting supernatants were combined, and proteins were precipitated by adding solid ammonium sulfate to achieve 10%, 25%, 40%, 50%, 60%, 80%, and 90% saturation, with each precipitation step continuing for 24 hours. Following each precipitation, samples were centrifuged (16,500 ×g, 40 minutes, 4 °C). The final supernatant was dialyzed against 10 mM Tris-HCl, pH 7.5. Protein concentration was determined spectrophotometrically using the Bradford assay. Bovine serum albumin was used as the standard.

### *2.3 Determination of RNA-Hydrolyzing Activity*

The relative RNA-hydrolyzing activity of holothurian proteins was assessed by monitoring the cleavage of fluorescently labeled ribooligonucleotides (5′-Flu-$(pA)_{23}$ and 5′-Flu-miR-aja-1715-5p). Standard 10-µL reaction mixtures contained 50 mM appropriate pH buffer, 0.025 mg/mL ribooligonucleotide, and 0.0025–0.3 mg/mL protein fraction. For assays with EDTA and metal ions, the 10 µL reaction mixture consisted of a 50 mM buffer (pH 5.0 or 6.0), 0.025 mg/mL ribooligonucleotide, 0.0025–0.01 mg/mL protein fraction, and either EDTA or metal salts ($MgCl_2$, $CaCl_2$) at concentrations of 1.0, 5.0, 10, 50, or 100 mM. All reactions were incubated at 37 °C for 30 minutes and terminated by adding 10 µL denaturing buffer (8 M urea, 0.025% xylene cyanol). Reaction products were separated by electrophoresis in 20% polyacrylamide gels (AA:bisAA ratio 29:1) containing 8.0 M urea. Hydrolysis product identification was performed using an alkaline hydrolysis ladder. The 10-µL ladder reaction contained 10% 0.5 M bicarbonate buffer (pH 9.5; 0.5 M sodium carbonate,

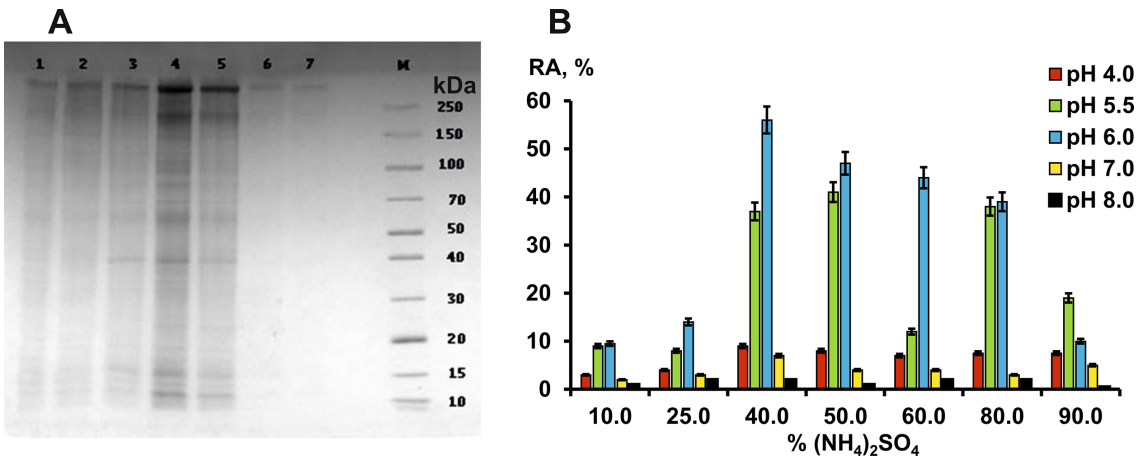


**Fig. 1. Electrophoretic analysis of protein fractions from the *E. fraudatrix* sea cucumber homogenate and the pH dependence of their relative RNase activity.** (A) SDS-PAGE of proteins fractions obtained by ammonium sulfate precipitation at 10%, 25%, 40%, 50%, 60%, 80%, and 90% saturation, (lane 1–7), respectively. Lane M – molecular weight markers. (B) Relative RNase activity of the fractions at different pH values (4.0–9.0), using 5′-Flu-$(pA)_{23}$ as a substrate. Results are shown as mean ± SEM from three experiments.

0.5 M sodium bicarbonate) and 0.05 mg/mL ribooligonucleotide. This marker reaction was incubated at 90 °C for 15 minutes, cooled on ice, and stopped with 10 µL denaturing buffer. Samples (10 µL) were loaded per lane, and electrophoresis was conducted at 800 V for approximately 1.5 hours. Relative activity was quantified by comparing band intensities of substrates and products, normalized to the no-protein control, using ImageQuant v5.2 (Molecular Dynamics World Headquarters, Sunnyvale, CA, USA) software.

### *2.4 Chromatographic Separation of Sea Cucumber Proteins*

The 50% ammonium sulfate-precipitated protein fraction from *Eupentacta fraudatrix* was loaded onto a Q Sepharose column (200 × 10 mm) pre-equilibrated with 20 mM Tris-HCl (pH 8.8). The column was washed with the same buffer until optical absorption returned to baseline. Bound proteins were eluted with a linear NaCl gradient (0 to 1 M) in 20 mM Tris-HCl (pH 8.8). Collected fractions were dialyzed overnight against 10 mM Tris-HCl (pH 8.8) at 4 °C.

The protein fraction corresponding to Peak B (see below section 3.4) from Q Sepharose chromatography was subsequently subjected to gel filtration chromatography on a Superdex 75 column (320 × 15 mm). The column was equilibrated with TBS buffer (20 mM Tris-HCl, pH 7.5, 0.15 M NaCl), and elution was performed with the same buffer. Resulting fractions were dialyzed against 10 mM Tris-HCl (pH 7.5) overnight at 4 °C.

### *2.5 Analysis of RNA-Hydrolyzing Activity in Situ*

Proteins were separated by electrophoresis in a gradient SDS-polyacrylamide gel containing yeast RNA (37 µg/mL). The stacking gel consisted of 4% acrylamide (AA:BisAA ratio = 29:1), 125 mM Tris-HCl (pH 6.8), and 0.1% SDS, while the separating gel contained a 4–18% acrylamide gradient (AA:BisAA ratio = 40:1), 375 mM Tris-HCl (pH 8.8), and 0.1% SDS. Protein samples (10–20 µg) were incubated in loading buffer (50 mM Tris-HCl, pH 6.8; 1% SDS; 10% glycerol; 0.001% bromophenol blue) at 25 °C for 2–3 minutes. Electrophoresis was performed at 100 V for 2.5 hours at 25 °C in 25 mM Tris-glycine buffer (pH 8.3) containing 0.1% SDS. Following electrophoresis, the gel was incubated in 2.0 M urea for 1 hour at 20–25 °C to renature proteins, followed by washing with distilled water for 1 hour (5–6 changes). To detect RNase activity, the gel was incubated in reaction buffer (20 mM Tris-HCl, pH 5.5; 1.0 mM EDTA) at 37 °C for 20 hours. The reaction time was optimized in preliminary experiments to yield ribonuclease activity bands of suitable intensity for densitometric analysis. Positive and negative controls (RNase A and bovine serum albumin) were included during method development but are not presented in the final results**.** The gel was then stained with 0.5 µg/mL ethidium bromide for 10 minutes. Relative RNase activity was quantified by measuring the intensity of dark zones (indicating RNA hydrolysis) against the background ethidium bromide fluorescence, with the highest activity value set as 100%. Analysis was performed using Image Lab v6.1 software. Finally, the gel was stained with Coomassie Blue R-250 (MP Biomedicals, Santa Ana, CA, USA) for total protein visualization.

## 3. Results

### *3.1 Isolation of Protein Fractions From the E. fraudatrix Sea Cucumber Homogenate*

Protein fractions from the sea cucumber *E. fraudatrix* homogenate, prepared as described in Section 2.2, were analyzed by electrophoresis on a gradient (4–18%) SDS-polyacrylamide gel (SDS-PAGE). As shown in Fig. 1A, the

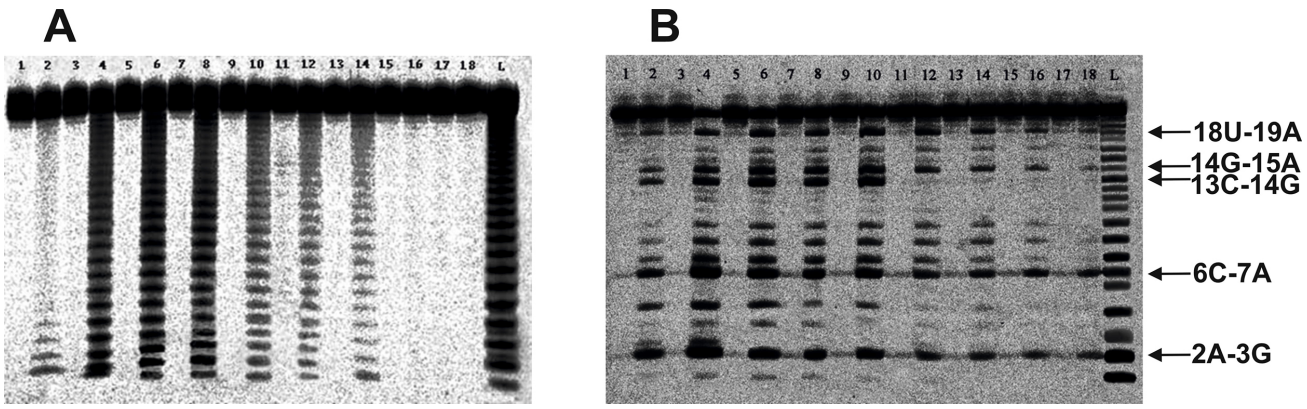


**Fig. 2. Electrophoretic analysis of RNase activity in the 50% ammonium sulfate fraction from the *E. fraudatrix* sea cucumber homogenate.** (A) Substrate: 5′-Flu-$(pA)_{23}$. Lanes: L – RNA molecular weight markers; odd-numbered lanes (1, 3, 5, 7, 9, 11, 13, 15, 17) – no-protein-controls at pH 4.5, 5.0, 5.5, 6.0, 6.5, 7.0, 7.5, 8.0, and 8.5, respectively; even-numbered lanes (2, 4, 6, 8, 10, 12, 14, 16, 18) – assays with the protein fraction at corresponding pH values. (B) Substrate: 5′-Flu miR-aja-1715-5p. Lane numbering scheme identical to A.

fraction precipitated at 50% ammonium sulfate saturation demonstrated the highest protein content.

### *3.2 Analysis of RNA-Hydrolyzing Activity in Protein Fractions From the E. fraudatrix Sea Cucumber Homogenate*

The RNase activity of various protein fractions from the *E. fraudatrix* homogenate was investigated using both a nonspecific homoribooligonucleotide, 5′-Flu-$(pA)_{23}$, and a specific miRNA, 5′-Flu miR-aja-1715-5p (a miRNA from the sea cucumber *Apostichopus japonicus*). The relative RNA-hydrolyzing activity was determined by measuring the hydrolysis of the fluorescently labeled ribooligonucleotide by holothurian proteins across a range of pH values. Each ammonium sulfate fraction (10, 25, 40, 50, 60, 80, and 90% saturation) was assayed for RNase activity at pH 4.0, 5.5, 6.0, 8.0, and 9.0. As shown in Fig. 1B, most protein fractions exhibited RNA-hydrolyzing activity. The highest RNase activity was observed in the 40%, 50%, 60%, and 80% ammonium sulfate fractions. The total protein content in the different fractions was estimated based on electrophoretic analysis. The 50% fraction contained 1.5 to 3 times more protein than the others. Since this fraction exhibited the highest protein content (Fig. 1A) and demonstrated maximal ribonuclease activity (Fig. 1B), it was selected for further investigation.

The RNA-hydrolyzing activity of the 50% ammonium sulfate fraction was further characterized across an extended pH range (4.0, 5.5, 6.0, 6.5, 7.0, 7.5, 8.0, 8.5, 9.0), with a comparative analysis of its activity towards the generic substrate 5′-Flu-$(pA)_{23}$ and the specific 5′-Flu miR-aja-1715-5p (Fig. 2A,B). Furthermore, the cleavage sites within the 5′-Flu miR-aja-1715-5p oligoribonucleotide were identified. As shown in Fig. 2B, the primary hydrolysis sites were located between 2A-3G, 6C-7A, 13C-14G, 14G-15A, and 18U-19A.

Analysis of the data presented in Fig. 3A reveals that the maximum hydrolysis level of 5′-Flu-$(pA)_{23}$ occurs at pH 6.0, whereas the highest activity for the specific miRNA substrate is observed at pH 5.0. Next, we investigated the EDTA and metal ions dependence of the RNase activity in the 50% ammonium sulfate fraction (substrates: 5′-Flu-(pA)23 and 5′-Flu-miR-aja-1715-5p). The enzymatic activity of the protein fraction under study decreased with increasing concentrations of both $Mg^{2+}$ and $Ca^{2+}$, as well as EDTA, for both substrates (Fig. 3B–D). Notably, the degree of substrate hydrolysis was approximately 25% higher for 5′-Flu-miR-aja-1715-5p compared to the non-specific substrate when equivalent amounts of EDTA or metal ions were added. This indicates that the ribonuclease activity in the 50% saturation homogenate fraction is dependent on metal ions.

### *3.3 Chromatographic Separation of E. fraudatrix Proteins by Ion Exchange Chromatography*

The protein fraction obtained by 50% ammonium sulfate precipitation was further separated using ion-exchange chromatography on a Q Sepharose column at pH 8.8. Elution was performed by applying a linear salt gradient (from 0 to 1.0 M NaCl). The resulting chromatographic profile is presented in Fig. 4A.

Chromatographic separation revealed that the majority of proteins did not bind to the sorbent (Peak A). Proteins eluted with a linear NaCl gradient separated into two distinct peaks (Fig. 4A). RNase activity of all fractions obtained from the chromatography was measured at pH 6.0 using two substrates: 5′-Flu-$(pA)_{23}$ and 5′-Flu-miR-aja-1715-5p. The highest hydrolytic activity was associated with Peak B, while the starting sample showed moderate activity. In contrast, the fraction containing proteins that did not bind to the sorbent (Peak A) exhibited minimal hydrolysis (Fig. 4B). Furthermore, the analyzed fractions demon-

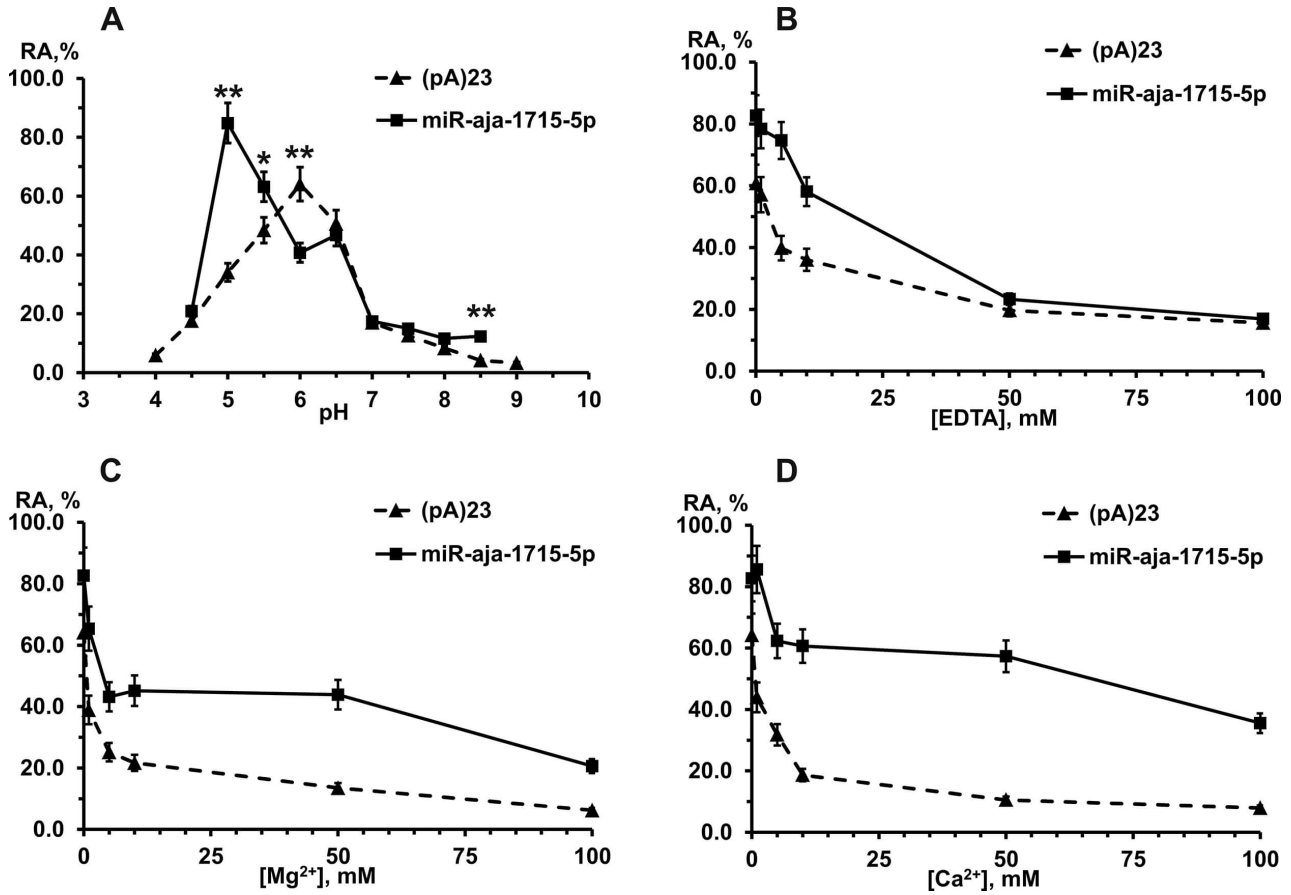


**Fig. 3. Relative RNase activity of the 50% ammonium sulfate protein fraction from the sea cucumber *E. fraudatrix* as a function of pH (A) EDTA (B), $Mg^{2+}$ (C) and $Ca^{2+}$ (D) concentration.** Results are shown as mean ± SEM from three experiments. In the case of pH dependence (A), the significance of differences was calculated at each point using Welch's *t*-test. $*p < 0.05$, $**p < 0.01$.

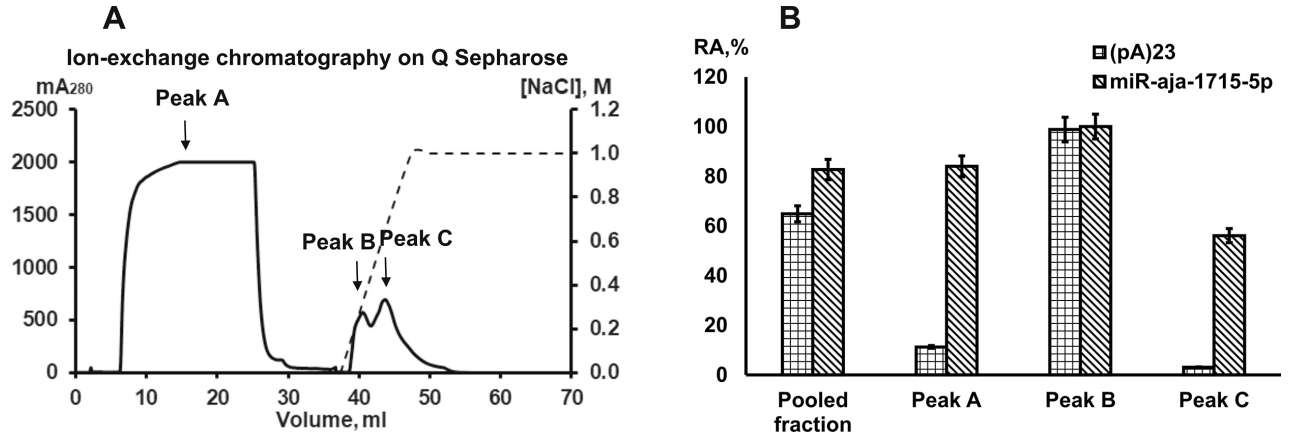


**Fig. 4. Chromatographic separation of homogenate proteins on Q Sepharose and RNase activity profile of proteins from the *E. fraudatrix* sea cucumber homogenate.** (A) Elution profile of the 50% ammonium sulfate fraction on a Q Sepharose column using a NaCl concentration gradient. (B) Relative RNase activity of the chromatographic fractions measured using 5′-Flu-$(pA)_{23}$ and 5′-Flu-miR-aja-1715-5p as substrates. Results are shown as mean ± SEM from three experiments.

strated a significant difference in their ability to hydrolyze the oligoA substrate, whereas their activity against 5′-Flu-miR-aja-1715-5p was comparable.

Subsequently, the RNase activity of the obtained fractions was analyzed *in situ* using a gradient (4–18%) SDS-PAGE at pH 5.5, with yeast tRNA as the substrate. Relative RNase activity was quantified based on the intensity of

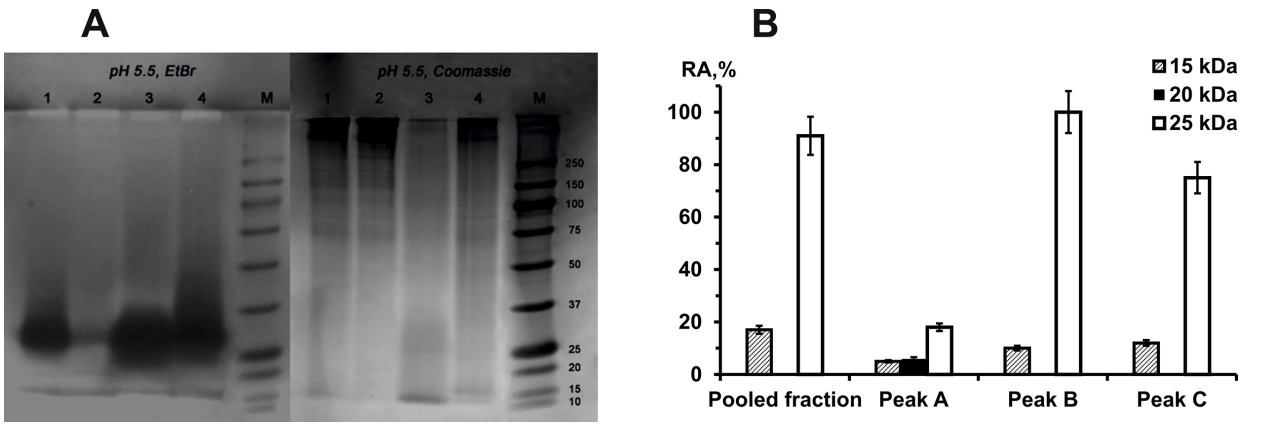


**Fig. 5. Analysis of RNase activity in protein fractions obtained by chromatographic separation using the *in situ* method.** (A) Gel electrophoresis analysis: Lane 1 – 50% precipitation fraction before separation; Lane 2 – unbound proteins, Peak A; Lane 3 – Peak B; Lane 4 – Peak C; M – protein molecular weight markers; pH 5.5, substrate – yeast tRNA. The gel was stained with ethidium bromide (left) and Coomassie (right). (B) Quantification of RNase activity obtained by the *in situ* method. The activity of the most active protein was set as 100%. Results are shown as mean ± SEM from three experiments.

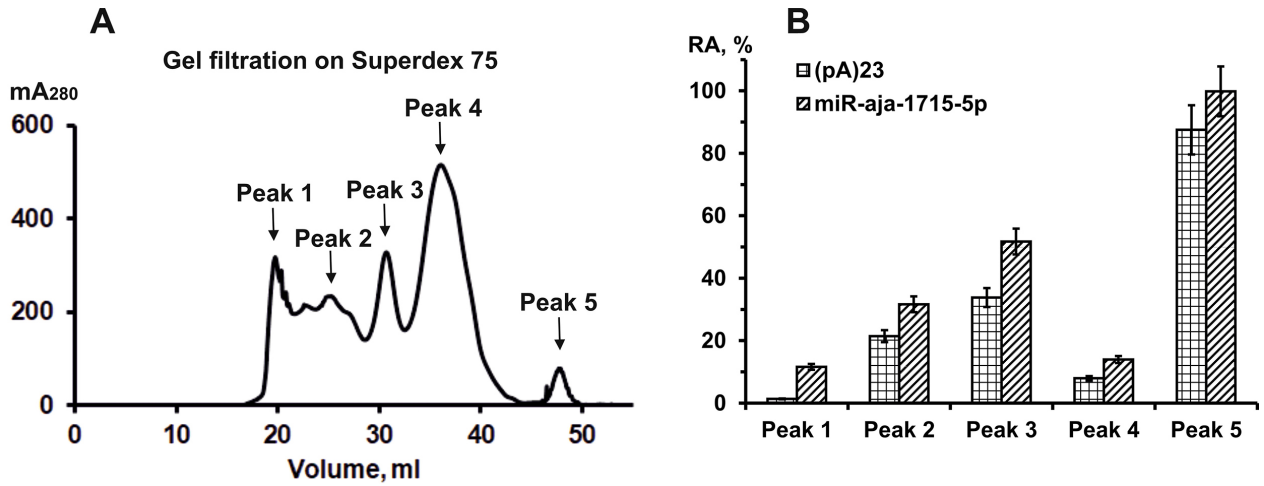


**Fig. 6. Gel filtration separation of *E. fraudatrix* proteins and RNase activity of the obtained fractions.** (A) Gel filtration profile of Peak B proteins obtained by ion-exchange chromatography of the 50% fraction (see Fig. 4A) on a Superdex 75 column. (B) Relative RNase activity (RA) of the resulting protein fractions. Results are shown as mean ± SEM from three experiments.

dark zones (absence of ethidium bromide, EtBr). As shown in Fig. 5A, at least two bands exhibiting ribonuclease activity, with apparent masses of approximately 25 and 15 kDa, were detected in all fractions. Moreover, the fraction with no affinity for the sorbent (Peak A) contains a ribonuclease with an apparent mass of approximately 20 kDa, which exhibits low activity under these conditions and is not detectable by Coomassie gel staining. The comparative diagram (Fig. 5B) reveals that the highest ribonuclease activity in each fraction is associated with the band corresponding to a ~25 kDa protein. This activity is maximal in the pooled fraction and in Fraction B. The ribonuclease activity associated with the ~15 kDa band is comparable across all fractions. For the non-binding fraction, the activity of both the ~25 kDa and ~15 kDa bands is minimal and similar to the activity level of the ~20 kDa band.

### *3.4 Chromatographic Separation of E. fraudatrix Proteins by Gel Filtration*

Since ion-exchange chromatography failed to resolve individual proteins, further separation was performed using gel filtration on a Superdex 75 matrix (Fig. 6A). At this stage, we aimed to investigate proteins with affinity for Q-Sepharose, i.e., those from fractions B and C. Since fraction B proteins demonstrated the highest ribonuclease activity in hydrolyzing the non-specific homoribooligonucleotide 5′-Flu-$(pA)_{23}$ (Fig. 4A,B), this fraction was selected for further analysis. The separation yielded five protein peaks, and the RNase activity of each was measured using 5′-Flu-$(pA)_{23}$ and 5′-Flu-miR-aja-1715-5p as substrates at pH 6.0. The highest enzymatic activity was observed in the fifth peak. Interestingly, in this case, the extent of hydrolysis for the non-specific homoribooligonucleotide was nearly iden-

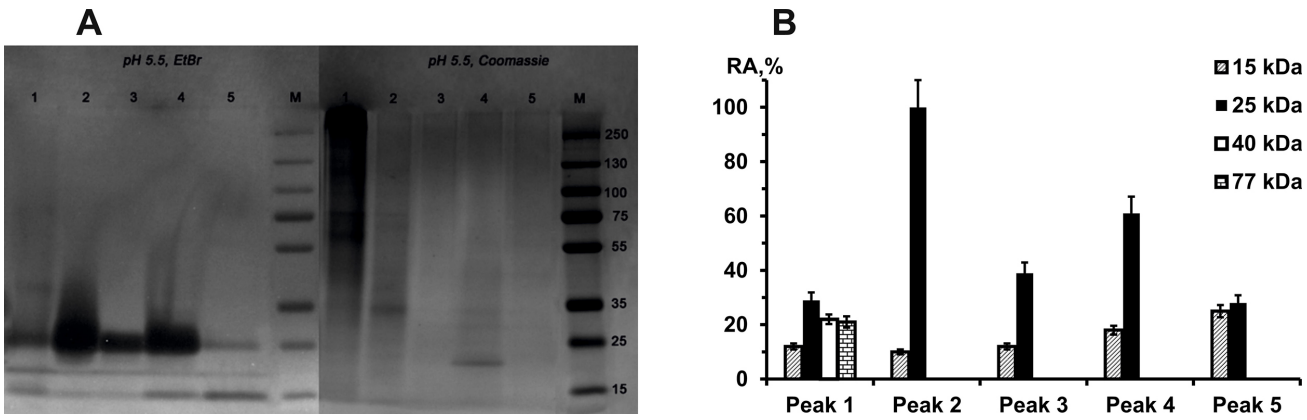


**Fig. 7. Analysis of RNase activity in protein fractions separated on Superdex 75 using the *in situ* method.** (A) Gel electrophoresis analysis: Lanes 1–5 correspond to Peaks 1–5; M – protein molecular weight markers. Conditions: pH 5.5, substrate – yeast tRNA. Gels were stained with ethidium bromide (left) and Coomassie Blue (right). (B) Quantification of RNase activity determined by the *in situ* method. The activity of the most active protein was set as 100%. Results are shown as mean ± SEM from three experiments.

tical to that observed for 5′-Flu-miR-aja-1715-5p (Fig. 6B).

Subsequent analysis of RNase activity in the obtained fractions was performed *in situ* using a gradient (4–18%) SDS-PAGE at pH 5.5 with yeast tRNA as the substrate (Fig. 7A). As with the previous separation step, all fractions exhibited at least two ribonuclease-active bands with masses of approximately 25 and 15 kDa. The band at ~25 kDa demonstrated the highest activity, yet it was not detectable by Coomassie gel staining. Furthermore, fraction corresponding to Peak 1 contains low-activity RNases with apparent molecular masses of approximately 40 kDa and 77 kDa under these experimental conditions, which were also undetectable by Coomassie staining. The comparative diagram (Fig. 7B) indicates that the highest ribonuclease activity in each fraction is associated with the ~25 kDa protein band, with peak activity observed in the Peak 2. The activity corresponding to the ~15 kDa band is maximal in the Peak 5. The ribonuclease activities of the bands with apparent masses of ~40 and ~77 kDa are comparable to each other and to that of the ~15 kDa band.

Table 1 summarizes the RNase activities in each fraction obtained from the two separation steps that hydrolyze yeast tRNA. These steps include: (1) ion-exchange chromatography of the 50% ammonium sulfate precipitate from the *E. fraudatrix* homogenate (Figs. 4,5), and (2) gel filtration of Peak B proteins obtained after the initial ion-exchange chromatography (Figs. 6,7).

## 4. Discussion

As previously demonstrated, the stable protein complex from the *Eupentacta fraudatrix* sea cucumber homogenate exhibits DNase and protease activities [27,28]. Holothurians are known for their regenerative capabilities, suggesting their proteins may possess diverse enzymatic functions. Furthermore, catalytic activities may manifest when individual proteins form stable complexes, whereas isolated proteins may remain inactive [29]. For *E. fraudatrix*, data on individual proteins are scarce, and no information on their RNase activity has been available. This study aimed to investigate this activity by isolating RNA-hydrolyzing proteins.

Protein fractions were obtained by precipitating the whole-organism homogenate of *E. fraudatrix* with ammonium sulfate at concentrations of 10%, 25%, 40%, 50%, 60%, 80%, and 90% saturation. Substrates included the non-specific homoribooligonucleotide 5′-Flu-$(pA)_{23}$ and the specific miRNA 5′-Flu-miR-aja-1715-5p (derived from the sea cucumber *Apostichopus japonicus*). The latter species is widely consumed and cultivated in Eastern countries, leading to the isolation and characterization of its miRNAs [30]. Although the functions of most miRNAs remain unconfirmed, their differential expression in abnormal physiological states implies functional roles in relevant processes. The expression level of miR-aja-1715-5p increases over 3000-fold in the regenerating intestine of *A. japonicus* compared to normal tissue, though its expression in *E. fraudatrix* has not been analyzed. We selected miRNA data from the sea cucumber *A. japonicus* as a reference for our analysis due to the known evolutionary conservation of key miRNA families within the phylum Echinodermata. Numerous comparative genomic studies confirm that fundamental miRNAs regulating development, cell cycle, and apoptosis (e.g., the *let-7* , *miR-10*, *miR-100*, and *miR-124* families) are highly conserved among echinoderms and exhibit similar expression patterns and functions [31,32]. Although species-specific differences in miRNA repertoires exist, utilizing annotated data from this well-established model species allows us to formulate informed hypotheses about the potential RNA targets of RNases in the context of *E. fraudatrix* biology. The reaction with 5′-Flu-$(pA)_{23}$ enabled initial assessment of RNase activity independent of ribooligonucleotide se-

**Table 1. RNases from the *E. fraudatrix* sea cucumber homogenate*.**

| | 15 kDa | 20 kDa | 25 kDa | 40 kDa | 77 kDa | In total |
|---|---|---|---|---|---|---|
| Pooled fraction (50%)** | + | – | + | – | – | 2 |
| Peak A (Fig. 4) | + | + | + | – | – | 3 |
| Peak B (Fig. 4) | + | – | + | – | – | 2 |
| Peak C (Fig. 4) | + | – | + | – | – | 2 |
| Peak 1 (Fig. 6) | + | – | + | + | + | 4 |
| Peak 2 (Fig. 6) | + | – | + | – | – | 2 |
| Peak 3 (Fig. 6) | + | – | + | – | – | 2 |
| Peak 4 (Fig. 6) | + | – | + | – | – | 2 |
| Peak 5 (Fig. 6) | + | – | + | – | – | 2 |

*Summary of ribonuclease-active bands detected by *in situ* assay at all stages of homogenate chromatographic purification. Apparent molecular masses determined by electrophoretic analysis are provided.

**Pooled fraction refers to proteins from the *E. fraudatrix* homogenate precipitated with 50% ammonium sulfate. Peaks A–C represent fractions collected after ion-exchange chromatography (Fig. 4). Peaks 1–5 correspond to fractions obtained by subsequent gel-filtration chromatography (Fig. 6).

quence, while hydrolysis of the hetero-oligoribonucleotide allowed detailed study of RNA cleavage mechanisms, including sequence-dependent effects. The 50% ammonium sulfate fraction showed the highest RNase activity, with pH optima at 5.0 and 6.0 for 5′-Flu-miR-aja-1715-5p and 5′-Flu-$(pA)_{23}$, respectively (Figs. 2,3). The specific substrate was hydrolyzed more efficiently, with five cleavage sites identified.

For the sea cucumber *E. fraudatrix*, data on ribonucleases are lacking. However, in other echinoderms—sea stars and sea urchins—RNases with a similar pH optimum (5.0–5.5) have been identified [9,10]. The detection of multiple forms of ribonuclease activity with distinct pH optima (5.0 and 6.0) in *E. fraudatrix* tissues may be attributed to several factors. If these activities represent different enzymes with distinct substrate specificities, they likely have different intracellular localizations and, consequently, biological functions. Activity with an optimum at pH 5.0 is characteristic of lysosomal ribonucleases, which are involved in RNA degradation under acidic conditions. In contrast, activity with an optimum at pH 6.0, closer to the neutral pH of the cytosol, may suggest an enzyme involved in more specific regulatory pathways, such as RNA processing or mRNA stability control. If both substrates are cleaved by a single enzyme, the observed shift in pH optimum for the ribonuclease activity indicates that the enzyme's ionizable groups involved in substrate binding and/or catalysis differ for the two substrates. Such active-site plasticity would enable the enzyme to efficiently process a broad spectrum of nucleic acids by adapting its catalytic mechanism to the chemical nature of the substrate. From a biological perspective, this could reflect the enzyme's ability to perform different functions in cellular compartments with varying pH (e.g., lysosomes vs. cytosol).

The inhibition of ribonuclease activity upon addition of EDTA, as well as $Mg^{2+}$ and $Ca^{2+}$ ions, indicates metal ion dependence. It is well established that metal-dependent ribonucleases require divalent metal ions—typically $Mg^{2+}$, $Ca^{2+}$, $Ni^{2+}$, $Mn^{2+}$, $Zn^{2+}$, or $Co^{2+}$—for catalysis [33]. The observation that ribonucleases in the homogenate fractions are instead inhibited by $Mg^{2+}$ and $Ca^{2+}$ may be explained by several hypotheses. First, catalysis may require a different metal ion, possibly $Mn^{2+}$ or $Zn^{2+}$, as some RNases show a preference for these ions. Alternatively, a two- or three-metal catalytic mechanism may be involved. Furthermore, certain RNases, such as RNase H, are known to be inhibited by calcium ions [34], and a similar mechanism may apply here. It is also important to note that the 50% fraction is not a homogeneous ribonuclease preparation and likely contains several distinct RNases; thus, the observed inhibition profile may represent a superposition of activities from multiple enzymes. In any case, further experiments are required to fully elucidate this mechanism and determine which metal ion(s)—single or multiple—activate the identified ribonucleases.

To further characterize RNase activity, isolation of individual RNA-hydrolyzing proteins was necessary. Ion-exchange chromatography yielded three protein fractions; however, obtaining homogeneous preparations was not possible, as each fraction contained a mixture of proteins and exhibited at least two protein bands with ribonuclease activity (Fig. 5). RNA-hydrolyzing proteins were detected in all three fractions, but in this study, we proceeded to investigate only one of them. Undoubtedly, future work should focus on characterizing the remaining two fractions. Peak A, demonstrating the highest activity against both miR-aja-1715-5p and yeast RNA (Figs. 4,5), was selected for gel filtration, yielding five protein peaks with RNase activity. All obtained protein fractions were analyzed not

only for miRNA hydrolysis but also by in-gel activity assay. The *in situ* method simultaneously assesses relative activity and molecular masses: proteins are separated in a gel with copolymerized yeast tRNA substrate, and post-incubation, RNase activity is visualized as dark zones (no EtBr fluorescence) where tRNA has been hydrolyzed. The data presented in Table 1 show that the highest number of protein bands exhibiting yeast RNA hydrolysis is observed in two fractions: the unbound fraction from ion-exchange chromatography (Peak A, bands) and Peak 1 from Superdex 75 separation (4 bands).

Notably, two protein bands with ribonuclease activity (40 and 77 kDa) detected in Peak 1 after gel filtration were not observed in the original fraction of Peak B (Figs. 5,7), indicating enrichment of RNA-hydrolyzing proteins during purification. Electrophoretic analysis confirmed that Peak B primarily contained low-molecular-weight proteins, whereas Peaks 1–5 obtained after its gel filtration retained multiple proteins from the original 50% ammonium sulfate fraction. Peak 1 was rich in high-molecular-weight proteins, Peaks 2 and 4 contained several low-molecular-weight proteins, while Peaks 3 and 5 had minimal protein content detectable by electrophoresis. Most RNases were undetectable by Coomassie staining, reflecting high specific activity and challenges in obtaining homogeneous preparations.

Furthermore, this study has several limitations. First, the analysis was performed using whole-organism homogenates. Given that enzyme expression is often organ-specific, investigating RNases from isolated organs would likely yield more homogeneous protein preparations and provide clearer insights into their functions. Second, due to practical constraints, not all protein fractions obtained could be characterized, which inherently limits the comprehensiveness of the study. Third, the molecular masses of the RNases reported here are apparent values, as they were determined solely by electrophoretic mobility. We detected five distinct ribonuclease-active protein bands with different electrophoretic mobilities. To definitively confirm that each activity corresponds to a unique gene product, further studies—such as mass-spectrometric protein identification and primary structure analysis—are required.

The ribonucleases we identified may serve distinct cellular functions. Enzymes with a pH optimum of 5.0 may play a degradative role, potentially involved in defense against infection or in nucleotide recycling. In contrast, enzymes with a pH optimum of 6.0 could operate in endosomes or specialized secretory granules, participating in signaling pathways or regulated RNA processing rather than mere digestion. In the context of regeneration, these enzymes may facilitate the removal of damaged cells and extracellular matrix at the injury site, particularly during early stages characterized by intense cellular turnover. Their regulatory functions might also be critical for the coordinated tissue remodeling required for reparative growth. The presence of multiple RNases with different properties suggests they may be activated at distinct stages of the complex regenerative process. It is important to emphasize, however, that all proposed roles of these RNases in regeneration remain speculative and necessitate further in-depth investigation.

## 5. Conclusions

In summary, this work characterized the RNase activity of *E. fraudatrix* homogenate proteins, revealing pH dependence and substrate specificity. This work represents the first report on the biochemical properties of a ribonuclease from this holothurian species. Using an *in situ* activity assay, we identified five distinct protein bands that differ in electrophoretic mobility and exhibit ribonuclease activity. It has been shown that, in their key characteristics (pH optimum and molecular masses), the discovered RNases resemble those found in sea stars and sea urchins. This study provides a solid foundation for the further identification of these ribonucleases, which should include precise structural elucidation and functional characterization in intact and regenerating organisms.

## Availability of Data and Materials

The datasets used and/or analyzed during the current study are available from the corresponding author on reasonable request.

## Author Contributions

Conceptualization, GAN and SES; methodology, VAI and IAK; formal analysis, IAK and SES; investigation, VAI, SES, and IAK; resources, GAN; data curation, GAN; writing—original draft preparation GAN; writing—review and editing, GAN and SES; project administration, GAN; funding acquisition, GAN. All authors contributed to editorial changes in the manuscript. All authors read and approved the final manuscript. All authors have participated sufficiently in the work and agreed to be accountable for all aspects of the work.

## Ethics Approval and Consent to Participate

This study was conducted in accordance with the ethical standards of the Russian Federation and the fundamental principles of laboratory animal science (the 3Rs - Replacement, Reduction, and Refinement). According to Article 2 of Federal Law No. 498-FZ “On Responsible Treatment of Animals” (December 27, 2018), the provisions requiring approval from an ethics committee apply exclusively to work with vertebrate animals. As this research exclusively involved marine invertebrates (sea cucumbers) for which no such requirement exists under Russian law, and no endangered or protected species were used, formal approval from an ethics committee was not required.

## Acknowledgment

We gratefully acknowledge the staff of the Marine Experimental Station of the Pacific Institute of Bioorganic Chemistry, Far Eastern Branch of the Russian Academy of Sciences, and Pavel S. Dmitrenok for organizing the collection of adult *Eupentacta fraudatrix* sea cucumbers in Peter the Great Bay, Sea of Japan.

## Funding

This research was performed due to a grant from Russian State-funded budget project of ICBFM SB RAS 125012300658-9.

## Conflicts of Interest

The authors declare no conflicts of interest.

## References

[1] García-Arrarás JE, Lázaro-Peña MI, Díaz-Balzac CA. Holothurians as a Model System to Study Regeneration. Results and Problems in Cell Differentiation. 2018; 65: 255–283. https://doi.org/10.1007/978-3-319-92486-1_13.

[2] Dolmatov IY, Kalacheva NV, Tkacheva ES, Shulga AP, Zavalnaya EG, Shamshurina EV, et al. Expression of *Piwi*, *MMP*, *TIMP*, and *Sox* during Gut Regeneration in Holothurian *Eupentacta fraudatrix* (Holothuroidea, Dendrochirotida). Genes. 2021; 12: 1292. https://doi.org/10.3390/genes12081292.

[3] Girich AS, Isaeva MP, Dolmatov IY. Wnt and frizzled expression during regeneration of internal organs in the holothurian Eupentacta fraudatrix. Wound Repair and Regeneration. 2017; 25: 828–835. https://doi.org/10.1111/wrr.12591.

[4] Su F, Dolmatov IY, Wang T, Yang H, Ding K, Zhang L, et al. LncRNA-miRNA interplay regulate intestinal regeneration in the sea cucumber *Apostichopus japonicus*. Computational and Structural Biotechnology Journal. 2025; 27: 1383–1393. https://doi.org/10.1016/j.csbj.2025.03.047.

[5] Su F, Huo D, Yang H, Sun L. CircRNA8388 functions as the sponge for miR-2392 during intestinal regeneration in sea cucumber Apostichopus japonicus. International Journal of Biological Macromolecules. 2024; 274: 133302. https://doi.org/10.1016/j.ijbiomac.2024.133302.

[6] Bernstein E, Caudy AA, Hammond SM, Hannon GJ. Role for a bidentate ribonuclease in the initiation step of RNA interference. Nature. 2001; 409: 363–366. https://doi.org/10.1038/35053110.

[7] Hoffend NC, Magner WJ, Tomasi TB. The modulation of Dicer regulates tumor immunogenicity in melanoma. Oncotarget. 2016; 7: 47663–47673. https://doi.org/10.18632/oncotarget.10273.

[8] Braun T, Klepzig H, Herling M. AGO2 in T-prolymphocytic leukemia: its canonical and non-canonical deregulation and function. Oncotarget. 2023; 14: 395–397. https://doi.org/10.18632/oncotarget.28378.

[9] Motoyoshi N, Kobayashi H, Itagaki T, Inokuchi N. Amino acid sequence analysis and characterization of a ribonuclease from starfish Asterias amurensis. Journal of Biochemistry. 2016; 160: 131–139. https://doi.org/10.1093/jb/mvw017.

[10] Sanda A, Kiyomoto M, Iwama M, Ohgi K, Irie M. Marked changes in the ribonuclease activity of mature and immature gonads of sea urchins Hemicentrotus pulcherrimus and Anthocidaris crassispina. Biological & Pharmaceutical Bulletin. 2008; 31: 1659–1662. https://doi.org/10.1248/bpb.31.1659.

[11] Boyko AV, Girich AS, Tkacheva ES, Dolmatov IY. The Eupentacta fraudatrix transcriptome provides insights into regulation of cell transdifferentiation. Scientific Reports. 2020; 10: 1522. https://doi.org/10.1038/s41598-020-58470-0.

[12] Zavalnaya EG, Shamshurina EV, Eliseikina MG. The Immunocytochemical Identification of PIWI-Positive Cells during the Recovery of a Coelomocyte Population after Evisceration in the Holothurian Eupentacta fraudatrix (Djakonov et Baranova, 1958) (Holothuroidea: Dendrochirota). Russian Journal of Marine Biology. 2020; 46: 97–104. https://doi.org/10.1134/S106307402002011X.

[13] Lu TX, Rothenberg ME. MicroRNA. The Journal of Allergy and Clinical Immunology. 2018; 141: 1202–1207. https://doi.org/10.1016/j.jaci.2017.08.034.

[14] Huo D, Sun L, Li X, Ru X, Liu S, Zhang L, et al. Differential Expression of miRNAs in the Respiratory Tree of the Sea Cucumber *Apostichopus japonicus* Under Hypoxia Stress. G3 (Bethesda, Md.). 2017; 7: 3681–3692. https://doi.org/10.1534/g3.117.1129.

[15] Yang Z, Wu J. MicroRNAs and regenerative medicine. DNA and Cell Biology. 2007; 26: 257–264. https://doi.org/10.1089/dna.2006.0548.

[16] Ambros V. MicroRNA-mediated gene regulation and the resilience of multicellular animals. Postepy Biochemii. 2024; 70: 62–70. https://doi.org/10.18388/pb.2021_515.

[17] Ho PTB, Clark IM, Le LTT. MicroRNA-Based Diagnosis and Therapy. International Journal of Molecular Sciences. 2022; 23: 7167. https://doi.org/10.3390/ijms23137167.

[18] Sun H, Zhou Z, Dong Y, Yang A, Jiang J, Chen Z, et al. Expression analysis of microRNAs related to the skin ulceration syndrome of sea cucumber Apostichopus japonicus. Fish & Shellfish Immunology. 2016; 49: 205–212. https://doi.org/10.1016/j.fsi.2015.12.036.

[19] Sun H, Zhou Z, Dong Y, Yang A, Pan Y, Jiang J, et al. In-depth profiling of miRNA regulation in the body wall of sea cucumber Apostichopus japonicus during skin ulceration syndrome progression. Fish & Shellfish Immunology. 2018; 79: 202–208. https://doi.org/10.1016/j.fsi.2018.05.020.

[20] Sun L, Sun J, Li X, Zhang L, Yang H, Wang Q. Understanding regulation of microRNAs on intestine regeneration in the sea cucumber Apostichopus japonicus using high-throughput sequencing. Comparative Biochemistry and Physiology. Part D, Genomics & Proteomics. 2017; 22: 1–9. https://doi.org/10.1016/j.cbd.2017.01.001.

[21] Jiao R, Wu B, Han S, Cui D, Sun J, Zhao T, et al. miRn-3 inhibits cutaneous wound healing by targeting gelsolin in the sea cucumber Apostichopus japonicus. International Journal of Biological Macromolecules. 2024; 254: 127801. https://doi.org/10.1016/j.ijbiomac.2023.127801.

[22] Zhang Y, Shao Y, Lv Z, Li C. MiR-210 regulates coelomocyte proliferation through targeting E2F3 in Apostichopus japonicus. Fish & Shellfish Immunology. 2020; 106: 583–590. https://doi.org/10.1016/j.fsi.2020.08.036.

[23] Chen M, Zhang X, Liu J, Storey KB. High-throughput sequencing reveals differential expression of miRNAs in intestine from sea cucumber during aestivation. PloS One. 2013; 8: e76120. https://doi.org/10.1371/journal.pone.0076120.

[24] Huo D, Su F, Yang H, Sun L. Exosomal microRNAs regulate the heat stress response in sea cucumber Apostichopus japonicus. Ecotoxicology and Environmental Safety. 2023; 249: 114419. https://doi.org/10.1016/j.ecoenv.2022.114419.

[25] Tian Y, Shang Y, Guo R, Chang Y, Jiang Y. Salinity stress-induced differentially expressed miRNAs and target genes in sea cucumbers Apostichopus japonicus. Cell Stress & Chaperones. 2019; 24: 719–733. https://doi.org/10.1007/s12192-019-00996-y.

[26] Huo D, Sun L, Sun J, Zhang L, Liu S, Su F, et al. Sea cucumbers in a high temperature and low dissolved oxygen world: Roles of

miRNAs in the regulation of environmental stresses. Environmental Pollution (Barking, Essex: 1987). 2021; 268: 115509. https://doi.org/10.1016/j.envpol.2020.115509.

[27] Timofeeva AM, Kostrikina IA, Dmitrenok PS, Soboleva SE, Nevinsky GA. Very Stable Two Mega Dalton High-Molecular-Mass Multiprotein Complex from Sea Cucumber *Eupentacta fraudatrix*. Molecules (Basel, Switzerland). 2021; 26: 5703. https://doi.org/10.3390/molecules26185703.

[28] Timofeeva AM, Kostrikina IA, Dmitrenok PS, Soboleva SE, Nevinsky GA. Protease and DNase Activities of a Very Stable High-Molecular-Mass Multiprotein Complex from Sea Cucumber *Eupentacta fraudatrix*. International Journal of Molecular Sciences. 2022; 23: 6677. https://doi.org/10.3390/ijms23126677.

[29] Martinez E. Multi-protein complexes in eukaryotic gene transcription. Plant Molecular Biology. 2002; 50: 925–947. https://doi.org/10.1023/a:1021258713850.

[30] Zhang L, Song X, Hamel JF, Mercier A. Aquaculture, stock enhancement, and restocking. Developments in Aquaculture and Fisheries Science. In Hamel JF and Mercier A. The sea cucumber Apostichopus japonicus: History, biology and aquaculture, 289–322. Academic Press (Elsevier): London. 2015. https://doi.org/10.1016/B978-0-12-799953-1.00016-7.

[31] Warner JF, Lyons DC, McClay DR. Left-right asymmetry in the sea urchin embryo: BMP and the asymmetrical origins of the adult. PLoS Biology. 2012; 10: e1001404. https://doi.org/10.1371/journal.pbio.1001404.

[32] Liu C, Yuan J, Zhang X, Jin S, Li F, Xiang J. Clustering genomic organization of sea cucumber miRNAs impacts their evolution and expression. Genomics. 2021; 113: 3544–3555. https://doi.org/10.1016/j.ygeno.2021.08.003.

[33] Pang J, Guo Q, Lu Z. The catalytic mechanism, metal dependence, substrate specificity, and biodiversity of ribonuclease H. Frontiers in Microbiology. 2022; 13: 1034811. https://doi.org/10.3389/fmicb.2022.1034811.

[34] Rosta E, Yang W, Hummer G. Calcium inhibition of ribonuclease H1 two-metal ion catalysis. Journal of the American Chemical Society. 2014; 136: 3137–3144. https://doi.org/10.1021/ja411408x.